

# Cold matter trapping via slowly rotating helical potential.

A.Yu.Okulov\*

General Physics Institute of Russian Academy of Sciences Vavilova str. 38, 119991, Moscow, Russia

(Dated: March 8, 2011)

We consider a cold bosonic ensemble trapped by a helical interference pattern in the optical *loop* scheme. Two counter propagating Laguerre-Gaussian laser beams (LG) with a slightly detuned frequencies produce rotating helical potential provided their orbital angular momenta are counter directed. The small frequency difference required for helix rotation might be induced by Sagnac effect or rotational Doppler effect. The superfluid hydrodynamics is analysed for the large number of atoms trapped by a slowly rotating helical optical potential when the kinetic energy is much smaller than interaction energy. Thus Gross-Pitaevskii equation is solved in Thomas-Fermi approximation and in "paraxial approximation" valid for highly elongated trap. The wavefunction of ensemble may cover all the LG beam waist with up to  $100\mu\text{m}$  in diameter and about  $1000\mu\text{m}$  in length. The speed of axial translation is determined and angular momentum of interacting atomic cloud is evaluated. Two possible configurations of the atomic ensemble wavefunction  $\Psi$  are demonstrated. The requirements for the implementation of such superfluid flow inside rotating optical helix are formulated in brief.

PACS numbers: 37.10.Gh 42.50.Tx 67.85.Hj 42.65.Hw

## I. INTRODUCTION

The hydrodynamics of the sufficiently cold ( $T \sim 10^{-6}K$ ) bosonic ensemble trapped by optical potential  $V(\vec{r}, t)$  [1–3] follows to Gross-Pitaevskii equation [4]:

$$i\hbar \frac{\partial \Psi}{\partial t} = -\frac{\hbar^2}{2m} \Delta \Psi + V(\vec{r}, t) \Psi + \frac{4\pi\hbar^2 a_s}{m} |\Psi|^2 \Psi, \quad (1)$$

where  $m$  is the mass of atom. The interaction of atoms leads to the remarkable many-body effects governed by the sign and magnitude of the scattering length: the negative  $a_s$  reduces the energy of ensemble hence causes the mutual attraction of atoms, which results in formation of bright solitons in **1D** and collapse in higher dimensions. On the contrary at positive  $a_s$  atoms repel each other and dark solitons or vortices are formed. In the presence of periodic potential gratings [5]:

$$V(\vec{r}, t) \sim I(z, t) \sim \exp[-r^2] \cos[\delta\omega t - (k_f + k_b)z], \quad (2)$$

where  $r$  is a distance from propagation axis  $z$ ,  $\delta\omega = c \cdot (k_f - k_b)$  is a frequency difference of the counter-propagating  $z$ -paraxial laser beams with the opposite wavevectors  $|\vec{k}_{(f,b)}| \approx k_{(f,b)}$ , the many-body nonlinearity is the cause of nonlinear tunneling, self-trapping and other quantum interference phenomena [6]. For accelerated **1D** optical gratings when  $\delta\omega = \delta\omega \cdot t$ , i.e. in the non inertial reference frames [5] the interacting bosons demonstrate Bloch oscillations and Landau-Zener tunneling.

The trap composed of the optical vortices produces the more complex interference patterns. The  $\lambda/2$  spaced

toroidal traps formed by isolated counter propagating LG beams had been demonstrated for the single atom trapping and detection [7] along with the persistent condensate flows in toroidal beam waist of LG beam [8]. As is shown in Sec.II following to [9] the phase-conjugation of the backward reflected LG beam transforms the **1D** sinusoidal intensity grating into the truly **3D** helicoidal intensity pattern  $I(z, r, \theta, t)$  [10]:

$$I(z, r, \theta, t) \cong r^2 \exp[-r^2] \cos[\delta\omega t - (k_f + k_b)z + 2\theta], \quad (3)$$

where  $\theta$  is azimuthal angle. The key point in achieving this field configuration (Sec.III) is in the opposite orbital angular momenta (OAM) of the interfering LG beams [11–13]. Noteworthy the counter propagating Bessel beam vortices are also capable to confine an atomic ensemble into the helical and toroidal waveguides [14]. Nevertheless in this case a phase conjugation is a necessary condition implicitly assumed for the Bessel traps and LG traps as well.

An analogous interferometric configurations were used previously for polarization gradient cooling [15], when laser beams with counter directed *spin* angular momenta (circular polarizations) produced static helical grating for the atomic beam.

In the sec.III we analyze the optical angular momentum in the purely *linear* optical setup. This setup might be effective experimental tool for producing the phase conjugation of LG-beams and helical interference patterns (3) therein. The frequency splitting of the order of  $\delta\nu \cong 10^{-1-2}Hz$  of the counter propagating LG's in a typical table top *loop* setup might appear because of Sagnac effect due to the Earth rotation which have angular frequency  $\Omega_{\oplus} = 2\pi/86400$  [16]. The other possibility to make small detuning  $\delta\omega = 2\pi\delta\nu$  is in usage of the rotational Doppler effect [17]. In both cases such a frequency shift will be the cause of the slow rotation of the helical interference pattern around the propagation axis [9].

\*Electronic address: alexey.okulov@gmail.com;  
URL: <http://www.gpi.ru/~okulov>

In the sec.IV we show how this rotating helix trapping configuration might be utilized for studies of the superfluidity mechanisms. The question is whether the cold atomic ensemble will remain in the irrotational state or suddenly switched helical optical potential will impose to the atomic cloud a rotation in the some form. In this connection we describe two possible regimes of the condensate trapping by this slowly rotating potential. In both cases the kinetic energy of atomic ensemble is expected to be small compared to the interaction and trapping energies. Two solutions of the Gross-Pitaevskii equation [4] for the mean field  $\Psi$  of the sufficiently large atomic ensemble  $N \sim 10^{(9-12)}$  are derived in the Thomas-Fermi approximation (TFA) in Sec.IV. One solution obtained as a balance of the red-detuned optical potential attraction and self-defocusing due to positive  $a_s$  has atomic density  $\rho_{helix}$  perfectly collocated with rotating optical helix  $I(z, r, \theta, t)$ . In this case the rotating potential imposes rotation to superfluid. In sec.V the Landau criterion  $|\vec{V}| > \epsilon(\vec{p})/|\vec{p}|$  for the appearance of elementary excitations and superfluidity lost [18] is discussed for helical geometry.

The other solution has nonrotating density  $\rho_{fun}$  "funnel" profile with time-dependent phase. In this *rest* regime the momentum  $\langle p_z \rangle$  and angular momentum  $\langle L_z \rangle$  of trapped ensemble remain equal to zero despite the rotation of a trap.

In both regimes the large volume  $V_H \cong 2\pi D_0^2 Z_r / 4$  of macroscopically coherent atomic ensemble with the helical modulation of density is anticipated. The diameter of cloud is expected to fit the LG beam waist being in the range  $D_0 \sim 30 - 100 \mu m$ , the length of trap is about the Rayleigh range  $Z_r \sim D_0^2 / \lambda \sim 300 - 1000 \mu m$ , the helix pitch is within  $\lambda \sim 0.8 - 10.6 \mu m$  (fig. 1).

These analysis is complementary to already performed experiments on condensate dragging in a fast rotation of pancake (**2D**) traps [1]. It is already known that rotating triangular and square optical lattices are capable to pin the vortices of cold boson at the antinodes (under *blue* detuning) of the optical interference pattern, but the perfect collocation was not observed [19].

In the absence of rotation a deep optical lattice maintains the long range order of condensate, but when potential is ramped out the vortex-antivortex pairs emerge in accordance with the Berezinskii-Kosterlitz-Thouless scenario [2]. Strictly speaking the optical lattices also contain singularities placed at the nodes of interference pattern [20]. Thus in a certain situation the optical torque may turn atoms in rotation around zeros of optical field: this process is expected to produce stable vortex-antivortex atomic lattices. In this connection of a particular interest are the square lattices in the near field of the *cw* solid-state microchip lasers [20–22].

The other relevant mechanism of static vortex lattice is *hexagonal* lattice formation by interference of the three-way segmented nonrotating condensate [23].

The static optical lattices proved to be efficient as many-body phenomena simulators [24, 25]. For exam-

ple the trimerized optical **2D** kagomé lattices were used to study a low-temperature properties of fermion gases [26].

## II. HELICAL INTERFERENCE PATTERN

It is well known that interference of a two counter-propagating optical waves with a slightly different frequencies  $\omega_f, \omega_b$  produces a running sinusoidal intensity grating [6, 29]. For the equal wave amplitudes  $|\mathbf{E}_f|, |\mathbf{E}_b|$  and the phase difference  $\phi$  the distribution of the light intensity  $I(z, r, \theta, t)$  have the following form in cylindrical coordinates  $z, r, \theta, t$  collocated with a propagation axis  $z$ :

$$I(z, r, \theta, t) = |\mathbf{E}_f(z, r, \theta, t) + \mathbf{E}_b(z, r, \theta, t)|^2 \cong 2|\mathbf{E}_{(f,b)}|^2 [1 + \cos[(\omega_f - \omega_b)t - (k_f + k_b)z + \phi]], \quad (4)$$

where a self-similar variable  $\chi = (\omega_f - \omega_b)t - (k_f + k_b)z + \phi$  is responsible for the translation of the interference pattern along  $z$  axis with the *group* velocity  $V_z = (\omega_f - \omega_b)/(k_f + k_b)$ . Taking into account the transversal (in the plane  $(r, \theta)$ ) confinement of the light amplitudes  $\mathbf{E}_f, \mathbf{E}_b$  typical e.g. for a zeroth-order Gaussian beams :

$$\mathbf{E}_{(f,b)}(z, r, \theta, t) \approx |\mathbf{E}_{(f,b)}| \exp[-i\omega_{(f,b)}t \pm ik_{(f,b)}z] \exp[-\frac{r^2}{D_0^2(1 + iz/(k_{(f,b)}D_0^2))}], \quad (5)$$

where  $D_0$  - is a beam waist diameter, we see that the *roll* interference pattern (4) transforms into the sequence of equidistantly spaced rotationally invariant (in  $\theta$ ) *ellipsoids* picked up by propagation axis  $z$  [9]:

$$I(z, r, \theta, t) = |\mathbf{E}(z, r, \theta, t)|^2 = |\mathbf{E}_f(z, r, \theta, t) + \mathbf{E}_b(z, r, \theta, t)|^2 \cong 2|\mathbf{E}_{(f,b)}|^2 [1 + \cos[(\omega_f - \omega_b)t - (k_f + k_b)z]] \exp[-\frac{2r^2}{D_0^2(1 + z^2/(k_{(f,b)}^2 D_0^4))}], \quad (6)$$

provided that a visibility of pattern is good enough  $|\mathbf{E}_f| \cong |\mathbf{E}_b|$  [27]. For the higher-order propagation modes say Laguerre-Gaussian beams (LG) with azimuthal quantum number  $\ell$  and angular momentum  $\ell\hbar$  per photon [28]:

$$\mathbf{E}_{(f,b)}(z, r, \theta, t) \sim \frac{\mathbf{E}_{(f,b)} \exp[i(-\omega_{(f,b)}t \pm k_{(f,b)}z) \pm i\ell\theta]}{(1 + iz/(k_{(f,b)}D_0^2))^2} (r/D_0)^{|\ell|} \exp[-\frac{r^2}{D_0^2(1 + iz/(k_{(f,b)}D_0^2))}], \quad (7)$$

the interference pattern is different for LG reflected from conventional mirror and phase conjugating mirror. Backward reflection from conventional spherical mirror changes the topological charge of the LG [9], exactly in the same way as circular polarization of light changes from left to right and vice-versa in reflection [29]. In addition the intensity  $I_{tor}(z, r, \theta, t)$  vanishes on the beam

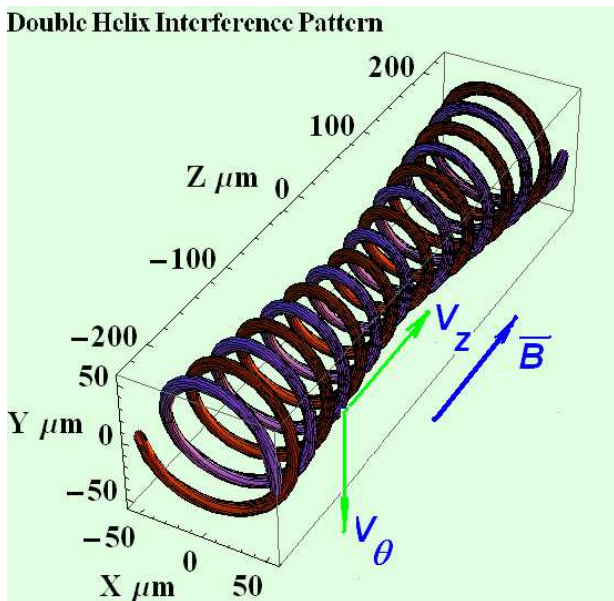


FIG. 1: The isosurface of the optical intensity  $I_{tw}$  and the Thomas-Fermi density  $\rho_{tw}$  of the cold atomic cloud in a helical optical dipole trap (9,30) (the scales are in  $\mu\text{m}$ , but longitudinal modulation of  $\lambda/2$  is enlarged). The spatial modulation of light intensity  $\cos(\delta\omega + 2kz \pm 2\ell\theta)$  (see equation (9)) is induced by the interference of counter-propagating LG waves with the opposite angular momenta. The pattern rotates with angular frequency  $\delta\omega$  as a "solid-body". This means that azimuthal speed of rotation is  $V_\theta = \delta\omega \cdot R$  while the axial speed, responsible for the helix pitch is equal to the group velocity of an overlapping LG's  $V_z = (\omega_f - \omega_b)/(k_f + k_b)$ . The isodensity surface  $\rho_{tw}$  of the helical atomic cloud rotates synchronously with the optical interference pattern. Magnetic field  $\vec{B}$  adjusts the scattering length  $a_s$  to balance the attractive potential by defocusing.

axis thus an interference pattern transforms into the sequence of the equidistant rotationally invariant *toroids* separated by  $\lambda/2$  interval:

$$I_{tor}(z, r, \theta, t) = \epsilon_0 c \frac{2|\mathbf{E}_{(f,b)}|^2 2^{(\ell+1)}}{\pi \ell! D_0^2} \times [1 + \cos[(\omega_f - \omega_b)t - (k_f + k_b)z]] \times (r/D_0)^{2|\ell|} \exp\left[-\frac{2r^2}{D_0^2(1 + z^2/(k_{(f,b)}^2 D_0^4))}\right]. \quad (8)$$

On the other hand the reflection from phase-conjugating mirror (PCM) [9, 30] does not change the topological charge of LG. As a result the expression for the interference pattern is slightly different [9, 12]:

$$I_{tw}(z, r, \theta, t) = \epsilon_0 c \frac{2|\mathbf{E}_{(f,b)}|^2 2^{(\ell+1)}}{\pi \ell! D_0^2} \times [1 + \cos[(\omega_f - \omega_b)t - (k_f + k_b)z + 2\ell\theta]] \times (r/D_0)^{2|\ell|} \exp\left[-\frac{2r^2}{D_0^2(1 + z^2/(k_{(f,b)}^2 D_0^4))}\right]. \quad (9)$$

The intensity also vanishes at LG axis  $z$  as  $r^{2|\ell|}$ , while a self-similar argument:

$$\chi = [(\omega_f - \omega_b)t - (k_f + k_b)z + 2\ell\theta], \quad (10)$$

where the azimuthal term  $2\ell\theta$  appears due to phase conjugation  $\mathbf{E}_b \sim \mathbf{E}_f^*$ , keeps the maxima of intensity at the two collocated helices each having  $\lambda$ -pitch separated from each other by  $\lambda/2$  interval (fig. 1). Thus we have the following strict correspondence between the *roll* interference pattern (6) and the helical interference pattern (9): the frequency difference  $\delta\omega = \omega_f - \omega_b$  is the cause of the translation of *rolls* with *group* velocity  $V_z = (\omega_f - \omega_b)/(k_f + k_b)$  of the wavetrain, produced by a sum of the two counter-propagating beams ( $\mathbf{E}_f + \mathbf{E}_b$ ) [5]. The  $\delta\omega$  is responsible for the rotation of *helices* with angular velocity  $\delta\omega = \omega_f - \omega_b$  as well. The rotation is the cause of the *pitch* of helical interference maxima along  $z$ -axis. Consequently there exists a perfect mechanical analogy between the *solid body* rotation of the helix described by formula (9) and an Archimedean screw. Namely the positive  $\delta\omega$  corresponds to the counter-clockwise rotation and this provides the *pitch* in positive  $z$  direction for *right* helices. On the other hand the negative  $\delta\omega$  means clockwise rotation. In this case ( $\delta\omega < 0$ ) the positive translation speed in  $z$  direction takes place for the *left*-handed helices. Evidently the change of the topological charge  $\ell$  changes the direction of helix translation  $\vec{V}_z$  due to alternation of the helix hand to the opposite one for fixed  $\delta\omega$ .

This mechanical analogy is useful for the analysis of the cold atoms motion in the helical trap. Virtually the velocity vector of the condensate fragment trapped and perfectly collocated with intensity maxima has two components  $\vec{V} = \vec{V}_z + \vec{V}_\theta$  (fig. 1). The axial component is a *group* velocity  $|\vec{V}_z| = (\omega_f - \omega_b)/(k_f + k_b)$  of the wavetrain, while the azimuthal component  $|\vec{V}_\theta| = (\omega_f - \omega_b) \cdot R$  is of kinematic nature. Such a *solid body* field of velocities is reminiscent to the rotation of a *classical* liquid together with rotating container [31, 32] where the angular velocity  $\delta\omega(r)$  is the  $r$ -independent constant. Noteworthy the *effective* field of velocities  $\vec{V} = \hbar\nabla\theta/m$  of the optical LG vortex (7) is of different nature and this effective velocity field is equivalent to those of quantum liquid composed of particles of mass  $m$  which have orbital angular momentum  $L_z = mV_\theta r = \ell\hbar$  independent of  $r$  [31]. As is well known the velocity  $\vec{V} = \hbar\nabla\theta/m$ ,  $V_\theta(r) \sim r^{-1}$  and the angular velocity  $\omega(r) \sim r^{-2}$  fields of the vortex inside quantum liquid have the point singularities at the vortex core ( $r \rightarrow 0$ ).

### III. LINEAR OPTICAL LOOP PHASE-CONJUGATION

The apparent topological difference of toroidal (8) and helicoidal (9) interference patterns is due to the mutual orientation of their orbital angular momenta. The

toroidal pattern appears when colliding photons have a parallel OAM's [7] while helicoidal pattern [9] arises for antiparallel OAM's. This follows from direct calculation of OAM for the  $\ell$ 'th order LG. The OAM is the expectation value of the angular momentum operator  $\hat{L}_z = -i\hbar[\vec{r} \times \nabla] = -i\hbar \frac{\partial}{\partial \theta}$  inside the interaction volume  $V \cong \pi R^2 Z_r$  [33, 34]:

$$\begin{aligned} \langle L_z \rangle_{(f,b)} &= \langle \Psi_{(f,b)}^\ell | \hat{L}_z | \Psi_{(f,b)}^\ell \rangle \\ &\sim \int_V (E_{(f,b)}^+)^* (-i\hbar[\vec{r} \times \nabla] E_{(f,b)}^+) d^3\vec{r} = \\ &\int (E_{(f,b)}^+)^* (-i\hbar \frac{\partial}{\partial \theta} E_{(f,b)}^+) r dr \cdot d\theta dz \sim \ell \hbar \frac{I_{(f,b)} V}{\hbar \omega_{(f,b)} c}, \end{aligned} \quad (11)$$

where  $I_{(f,b)} = \epsilon_0 c |\mathbf{E}_{(f,b)}|^2$  is the light intensity,  $\Psi_{(f,b)}^\ell = \sqrt{2\epsilon_0} E_{(f,b)}^+(z, r, \theta, t)$  is the macroscopic wavefunction of a single light photon inside a forward ( $f$ ) or backward ( $b$ ) LG wavetrains (7) with the winding number  $\ell$ . The retroreflector is placed apart from the interaction volume  $V$  located near  $z = 0$  plane within Rayleigh range  $Z_r < k_{(f,b)} D_0^2$  and the fields  $E_{(f,b)}^+$  are both calculated inside this volume (fig.2). The square modulus  $|\Psi_{(f,b)}^\ell|^2$  is a probability density for energy rather than for a particle (photon) location. This is a Sipe's single-photon wavefunction [35] which is proportional to the positive frequency part  $E_{f,b}^+$  of the counter-propagating fields. The usage of the nonrelativistic operators of the linear momentum ( $\hat{p} = -i\hbar\nabla$ ) and angular momentum ( $\hat{L}_z = -i\hbar \frac{\partial}{\partial \theta}$ ) is justified by the applicability of the paraxial approximation to the slowly diverging LG beams. In this particular paraxial case the spin-orbit coupling [36] may be neglected and the angular momentum of the photon is exactly decoupled to the spin and the orbital component:  $\hat{J} = \hat{S} + \hat{L}$ . The linear momentum expectation values  $\langle \vec{p} \rangle_{(f,b)}$  for the forward and backward LG's respectively are obtained in following way:

$$\begin{aligned} \langle p_z \rangle_{(f,b)} &= \langle \Psi_\ell | \hat{P} | \Psi_\ell \rangle \\ &\sim \int (E_{(f,b)}^+)^* (-i\hbar \nabla E_{(f,b)}^+) d^3\vec{r} = \\ &\int (E_{(f,b)}^+)^* (-i\hbar \frac{\partial}{\partial z} E_{(f,b)}^+) d^3\vec{r} \hbar k_{(f,b)} \frac{I_{(f,b)} V}{\hbar \omega_{(f,b)} c} \\ &\cong \pm N \hbar k_z, \end{aligned} \quad (12)$$

It follows from Maxwell equations that the expression for the classical momentum density of electromagnetic field is the *polar* vector  $\vec{P}$ , while angular momentum density  $\vec{M}$  is the *axial* vector [37]:

$$\vec{P}(z, r, \theta, t) = \epsilon_0 [\vec{E} \times \vec{B}]; \quad \vec{M}(z, r, \theta, t) = \epsilon_0 [\vec{r} \times [\vec{E} \times \vec{B}]] \quad (13)$$

By Ehrenfest theorem one might expect the identity of the classical and quantum mechanical calculations of the linear and angular momenta. The integration over LG interaction volume  $V$  containing cold atomic cloud gives

the classical momentum  $P_z$  of the incident and reflected LG's projected on  $z$ -axis:

$$\begin{aligned} P_{z(f,b)} &\cong \frac{\epsilon_0}{c} \int_0^{2\pi} d\theta \int_0^R r dr \int_{-Z_r}^{Z_r} [\vec{E} \times \vec{B}] dz \Big|_z \\ &\cong \pm I_{(f,b)} \cdot \pi R^2 \cdot Z_r / c^2, \end{aligned} \quad (14)$$

where  $2Z_r$  is the length of trapped cloud,  $R = D_0/2$  is the radius of helix. In a same way the classical angular momenta  $L_z$  of LG beams inside the interaction volume  $V \cong 2\pi R^2 Z_r$  projected on  $z$ -axis are:

$$\begin{aligned} L_{z(f,b)} &= \epsilon_0 \int_0^{2\pi} d\theta \int_0^R r dr \int_{-Z_r}^{Z_r} [\vec{r} \times [\vec{E} \times \vec{B}]] dz \Big|_z \\ &\cong \pm \ell \cdot I_{(f,b)} \cdot \pi R^2 \cdot Z_r / (c \omega_{(f,b)}). \end{aligned} \quad (15)$$

The ratio of the angular and linear momenta proved to be  $L_z/P_z \sim \ell c/\omega_{(f,b)}$  [37]. Consequently both classically and quantum mechanically when linearly polarized (with  $(\vec{S} = 0)$ ) LG-beam is retroreflected from conventional mirror, the *polar* vector of the optical momentum  $\vec{P}$  changes direction to the opposite one while the *axial* vector of the angular momentum  $\vec{J} = \vec{L}$  remains unchanged due to the isotropy of reflector [9]. Thus the topological charge  $\ell$  in (7) alters sign. The next reflection will change the topological charge once again due to the same reasons. From this follows that after an *even* number of reflections the topological charge will be conserved. Because LG is the eigenfunction of a free space parabolic wave equation it's propagation is self-similar in free space. The same holds for the passage through the smooth curved optical surfaces alike thin quasiparabolic lenses. In addition the LG's reflection from planar or smooth curved surfaces is self-similar too. Consequently the linear momentum and angular momentum conserve their mutual orientation (projection of angular momentum upon propagation axis, or momentum [33]) after the *even* number of reflections from isotropic optical elements.

In contrast to the conventional mirrors the wavefront reversing (PC) mirrors are essentially anisotropic optical elements [9, 11]. Due to the internal helical structures, e.g. acoustical vortices in SBS mirrors, the PC mirror turns the angular momentum of the incident beam to the opposite direction. Thus because the linear momentum  $\vec{P}$  is turned too, the mutual orientation of  $\vec{P}$  and  $\vec{L}$  is conserved and the topological charge  $\ell$  is not changed by an *ideal* PC mirror.

For the linear polarization, i.e. for zero-spin LG-photons with winding number  $\ell$ , the equivalence between *nonlinear* PC-mirrors, like Stimulated Brillouin mirrors, photorefractive mirrors, liquid crystal light valves etc. and topologically equivalent set of a *linear* optical elements may be achieved in a closed *loop* setup. The simplest conceivable configuration composed of plane mirrors, wavefront curvature compensating lenses and beam splitters is shown at fig.2. The goal of proposed setup is to counter-direct the splitted LG beams. The four

reflections look as a necessary minimum, because the incidence angles much above 45 degrees will enhance the effects of LG transformation and a small sliding of a beam along the reflecting surface [38] caused by unavoidable anisotropy of the mirror tilted with respect to the LG propagation axis. The auxiliary physical restrictions on this *loop* setup are in maintaining the path difference  $\Delta L$  of splitted LG's to be smaller than coherence length of trapping laser field ( $\Delta L \ll c \cdot \tau_{coh}$ ) inside the helical interference volume (the latter is located inside vacuum tube with cold atoms, see fig.2). The parabolic wavefront curvature due to the free-space propagation beam spread is to be compensated by parabolic (sufficiently thin) lenses shown at fig.2.

These restrictions upon coherence length, wavefront curvature and small frequency shift  $\delta\omega$  were already implemented successfully in experimental setups for trapping the cold atoms in a standing, moving and accelerating optical gratings [5]. Thus a *linear* optical loop setup outlined above provided the *even* number of reflections per a single loop roundtrip might be a practical equivalent of the nonlinear optical PC retroreflector [9, 12, 13].

Because of the Earth rotation having angular frequency  $\Theta_{\oplus}$  and the optical table rotation  $\Omega_{tab}$  the *Sagnac loop* phase shift to occur [16]:

$$\delta\vartheta = \frac{8\pi A \Omega_r}{c \cdot \lambda}, \quad (16)$$

where  $\Omega_r = \Theta_{\oplus} + \Omega_{tab}$  is angular speed of rotation of the laboratory frame,  $A$  is the square of the loop. This additional phase shift  $\delta\vartheta$  appears in the self-similar variable:

$$\chi = [(k_f + k_b)z + 2\ell\theta + \delta\vartheta], \quad (17)$$

resulting in the static phase shift in the interference pattern (9). Consequently the rotation of the *passive* loop will cause the static turn of the helical pattern, proportional to  $\Omega_r$ .

Alternatively the small frequency shift  $\delta\omega = \omega_f - \omega_b \approx 2\pi \cdot 10^{-(1-3)} rad/sec$  required to cause the helix rotation [9] might be induced by a frequency ramp [5] or via rotational Doppler shift which appears i.e. due to rotation of the half-wavelength plate [17]. Moreover there exists the possibility of obtaining the detuning  $\delta\omega$  of the counter-propagating optical LG beams due to the Sagnac effect in the optical *loop* with laser gain medium inside [16]:

$$\delta\omega = \frac{8\pi^2 A \Omega_r}{P \cdot \lambda}, \quad (18)$$

where  $P$  is the perimeter of the loop. On the other hand, the rotation  $\Omega_r$  of the *active* laser loop with an optical amplifier inside results in the slow rotation of the helical pattern with the angular frequency  $\delta\omega$  [13].

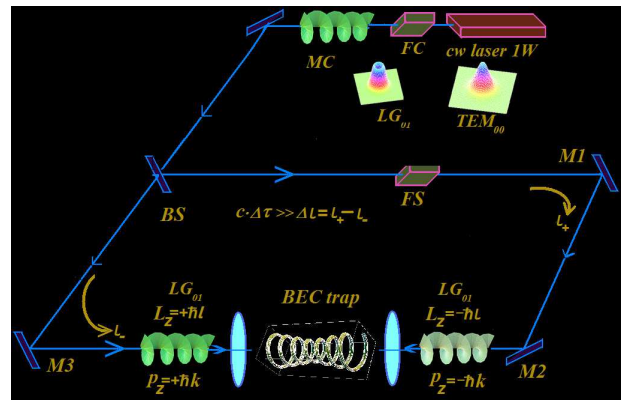


FIG. 2: The closed loop setup for producing the helical interference pattern. The CW laser emits fundamental mode which passes through Faraday isolator (FC). The mode-converter MC made of the two cylindrical lenses [37] transforms the fundamental Gaussian mode into LG beam with topological charge  $\ell$ . The beamsplitter BS changes the topological charge of the reflected beam to the opposite one and leaves the  $\ell$  unchanged for transmitted LG. After the even number of reflections both LG beams meet inside trap volume  $V$ . The path difference  $\Delta L = l_+ - l_-$  is assumed to be smaller than coherence length  $L_{coh} = c \cdot \tau$ , where  $\tau$  is the coherence time. The minimal amount of reflections for the in-plane geometry is required for turnover of the angular momentum  $L_z$  to the opposite one is equal 2. The clockwise beam  $l_+$  experiences two reflections at mirrors M1 and M2 after the passage through BS, the counterclockwise beam  $l_-$  after reflection from BS changes its OAM (and topological charge  $\ell$ ) once again at mirror M3. As a result both LG possess the opposite angular momenta ( $\hbar$  per photon) and produce helical interference pattern in trapping volume. The parabolic wavefront correcting elements are not shown. The frequency shifting FS box denotes symbolically the detuning of the counter-propagating beams  $\delta\omega$  caused by a frame rotation  $\Omega_r$  or frequency ramp, produced via i.e. rotational Doppler shift. For active *loop* FS designates the laser amplifier placed inside loop [16].

#### IV. MACROSCOPIC WAVEFUNCTIONS FOR A COLD BOSONS IN A RED-DETUNED HELICAL TRAPS.

Consider a bosonic cloud loaded in the helical interference pattern (9). The most relevant to this geometry experiment might be performed using the currently available cold atom setups. Let us consider a cloud prepared in an elongated trap [5] and subsequently released afterwards. The well elaborated procedure is to impose a periodic optical potential to study the Bloch oscillations, macroscopic Landau-Zener tunneling and Josephson effects [6, 24]. In our case the imposed optical potential is assumed to have the following *helical* form:

$$V_{opt}(z, r, \theta, t) = -\frac{Re[\alpha(\omega)]}{2\epsilon_0 c} I_{tw}(z, r, \theta, t),$$

$$\alpha(\omega) = 6\pi\epsilon_0 c^3 \frac{\Gamma / \omega_0^2}{(\omega_0^2 - \omega^2 - i(\omega^3 / \omega_0^2)\Gamma)}, \quad (19)$$

where  $\alpha(\omega)$  is the polarizability of atom, which is real, i.e.  $\alpha(\omega) \approx \text{Re}[\alpha]$  at large detunings from resonance  $\omega - \omega_0$ ,  $\Gamma = e^2\omega_0^2/6\pi\epsilon_0 m_e c^3$  is classical damping rate via radiative energy loss,  $m_e$  is electron mass,  $\epsilon_0$  is the dielectric constant of vacuum [3, 20]. For a low temperatures ( $T \cong 0$ ), *red* detuning  $\omega_0 - \omega_{f,b} > 0$  and when a number of trapped bosons  $N = \int |\Psi|^2 d^3\vec{r}$  is large enough, the Gross-Pitaevskii equation (GPE) for the macroscopic BEC wavefunction  $\Psi$  confined by the helical potential  $V_{opt}$  reads as:

$$i\hbar \frac{\partial \Psi(\vec{r}, t)}{\partial t} = \hat{H} \Psi(\vec{r}, t) = -\frac{\hbar^2}{2m} \Delta \Psi + V_{opt}(z, r, \theta, t) \Psi + \frac{4\pi\hbar^2 a_s(\vec{B})}{m} |\Psi|^2 \Psi, \quad (20)$$

where  $a_s(\vec{B}) = a_{bg}(1 + \Delta_B/(|\vec{B}| - B_F))$  is magnetic field dependent *s*-wave scattering length,  $a_{bg}$  is background value of  $a_s$ ,  $B_F$  and  $\Delta_B$  are the Feshbach magnetic induction and resonance width respectively,  $m$  is the mass of trapped bosons.

The helical trapping configuration offers a certain difficulties in searching the both the ground state  $\Psi_0$  and excited states. For the sake of preliminary analysis let look for the ultimately simplified solutions. Namely for the sufficiently large number of trapped atoms ( $N \cong 10^9-12$ ) the quantum pressure term which follows from the uncertainty principle ( $\hbar^2 \Delta \Psi / 2m \sim 0$ ) is small compared to the optical trapping and interaction terms (second and third terms in the right side of eq.(20)). Namely the standard criterion for the neglect of kinetic energy [4]:

$$\frac{E_{int}}{E_{kin}} \cong \frac{N \cdot a_{bg}}{a_{ho}}, \quad (21)$$

is replaced in our case to another one, where  $K_{int}$  is evaluated for the helical density profile  $|\Psi_{helix}|^2$  as:

$$\frac{E_{int}}{E_{kin}} \cong \left( \frac{N \cdot 2 \cdot \hbar^2}{m\lambda^2} \right)^{-1} \left( \frac{4\pi\hbar^2 a_s N^2 4\lambda}{m\pi D_0^4} \right) = \frac{8N \cdot a_s(\vec{B})\lambda^3}{D_0^4}, \quad (22)$$

here the "harmonic oscillator width" [4] equals to  $a_{ho} \cong \sqrt{\hbar/m\omega_z} \sim \lambda/2$  and the atomic density  $\rho = N/V_H$  was averaged over the above defined helical trap volume  $V_H = \pi D_0^2 Z_r / 2$ . According to (22) the ratio  $E_{int}/E_{kin}$  must be much more than unity for the most of the near infrared lasers  $\lambda = 0.8 - 1.5\mu m$ , under the standard focusing requirement  $D_0 \sim 10 - 100\mu m$  and under the experimentally achievable tuning of  $a_s(\vec{B})$  in the range  $\cong 1 - 100nm$  via Feshbach resonance. For the mid-infrared trapping at carbon dioxide lasing wavelength  $\lambda = 10.6\mu m$  the kinetic energy term  $E_{kin} = 2\hbar^2/m\lambda^2$  estimated by uncertainty principle is about 100 times smaller, so  $E_{int}$  and  $E_{dipole}$ :

$$E_{dipole} \cong N \cdot V_{opt} \cong -\frac{\vec{p} \cdot \vec{E}}{2} \cong \frac{-\alpha E^2 N}{2} \cong \frac{-\alpha I_{tw} N}{2\epsilon_0 c} = \frac{-e^2 I_{tw} N}{m_e \Delta\omega^2 2\epsilon_0 c}, \quad (23)$$

play a dominant role as well (where  $I_{tw}$  is the optical intensity of trapping beams,  $m_e$  is electron mass). We have used here the universal form of electric dipole transition applicable to alkali atoms with a few percent accuracy [3]:

$$\frac{\alpha E^2}{2} \cong \frac{e^2 E^2}{2m_e \cdot \Delta\omega^2}, \quad \Delta\omega = \omega_{f,b} - \omega_0 \quad (24)$$

Hence one might expect that a Thomas-Fermi approximation (TFA) is valid in our case when interaction is repulsive, i.e. for the positive  $a_s$  [4]. The magnitude and sign of the scattering length  $a_s$  are flexible parameters due to the externally applied magnetic induction  $\vec{B}$  for the alkali atoms alike *Li, Na, K, Rb, Cs* [24].

The following estimates will be done for simplicity in the vicinity of the LG-beam waist, i.e. within Rayleigh range, when  $z < k_{f,b} D_0^2$ . Consider first the following TFA wavefunction which satisfies the GPE (20):

$$\Psi_{fun}(z, r, \theta, t) \approx \Phi(r) \exp\left[-\frac{i\mu(r)t}{\hbar} + i\Phi(r)^2 \sin(\delta\omega t - 2k_z z + 2\ell\theta)\right], \quad (25)$$

where  $\mu(r)$  is a local (*r*-dependent) value of chemical potential defined as:

$$\mu(r) = 4\pi\hbar^2 a_s \Phi(r)^2 / m; \quad I_0 = 2\epsilon_0 c |\mathbf{E}_{(f,b)}|^2; \quad \Phi(r)^2 = \exp(-2r^2/D_0^2) \cdot (r/D_0)^{2|\ell|} \cdot \frac{\alpha(\omega) I_0}{2\epsilon_0 c \cdot \hbar \cdot \delta\omega}. \quad (26)$$

The wavefunction (25) is normalizable and fits the GPE by direct substitution. In particular the TFA density of atoms  $\rho_{fun}(z, r, \theta, t) = |\Psi_{fun}|^2 \approx \exp(-2(r/D_0)^2)/(r/D_0)^{2|\ell|}$  is (*z, t*)-independent "funnel" collocated with the optical helix  $I_{tw}(z, r, \theta, t)$ . The phase modulation of  $\Psi_{fun}$  has a maximum near the density maximum  $\rho_{fun}(z, r, \theta, t)$  and decreases down to zero on LG axis and outside the LG waist. The phase modulation has sinusoidal dependence on azimuthal angle  $\theta$ . The  $\Psi_{fun}$  is multiply valued function of  $\theta$ , so this solution might be of highly restricted interest only, in particular using  $|\Psi_{fun}|^2$  density profile for the evaluations of thermodynamical parameters of the cold ensemble, as other TF solutions are typically used [4].

The other solution in TF approximation is obtained for *r*-independent chemical potential  $\mu = const$ . In this regime the mean field wavefunction  $\Psi$  is a sum of the two phase-conjugated wavefunctions with the opposite topological charges  $\ell$ :

$$\Psi_{helix}(z, r, \theta, t) = \Psi_{\ell}(z, r, \theta, t) + \Psi_{-\ell}(z, r, \theta, t) \cong \Psi_{\pm\ell}(z=0) \cdot (r/D_0)^{|\ell|} \exp\left[-\frac{r^2}{D_0^2(1+iz/(k_{(f,b)}D_0^2))}\right] \left\{ \frac{\exp[-i\mu_f t/\hbar + ik_f z + i\ell\theta]}{(1+iz/(k_f D_0^2))^2} + \frac{\exp[-i\mu_b t/\hbar - ik_b z - i\ell\theta]}{(1+iz/(k_b D_0^2))^2} \right\}, \quad (27)$$

where the difference of the partial chemical potentials  $(\mu_f - \mu_b)$ , associated with the each of "counter-propagating" wavefunctions  $\Psi_\ell, \Psi_{-\ell}$  is adjusted to the frequency difference of counter-propagating optical fields  $(\mu_f - \mu_b)/\hbar = \delta\omega = \omega_f - \omega_b$ . The substitution of this TFA wavefunction into GPE gives the following link for parameters:

$$\rho_{helix}(z, r, \theta, t) = |\Psi_{helix}(z, r, \theta, t)|^2 = \frac{\mu - \alpha(\omega)I_{tw}(z, r, \theta, t)/2\epsilon_0 c}{g}, \quad (28)$$

where  $\mu = \mu_f \approx \mu_b$  is a constant ( $z, r, \theta, t$ -independent) value of chemical potential,  $g = 4\pi\hbar^2 a_s(\vec{B})/m$  is the interaction parameter. This equation means the quasiclassical restriction imposed on a homogeneity of chemical potential of the system in an external field  $V_{opt}$  [4]:

$$\mu_1[\rho_{helix}(z, r, \theta, t)] + \alpha(\omega)I_{tw}(z, r, \theta, t)/2\epsilon_0 c = \mu = const \quad (29)$$

obtained for the gas with the local value of the chemical potential  $\mu_1(\rho(\vec{r}, t)) = g\rho_{helix}$ . In accordance to this solution the density of the cold atomic ensemble  $\rho_{helix}(z, r, \theta, t)$  is perfectly correlated with the rotating optical helix potential  $I_{tw}(z, r, \theta, t)$  as depicted at fig.1:

$$\rho_{helix}(z, r, \theta, t) = \mu - \frac{\alpha(\omega)I_{tw}(z=0) \cdot [1 + \cos(\delta\omega t + 2kz \pm 2\ell\theta)]}{2\epsilon_0 c \cdot g (1 + z^2/(k^2 D_0^4))} \times (r/D_0)^{2|\ell|} \exp\left[-\frac{2r^2}{D_0^2(1 + z^2/(k_{(f,b)}^2 D_0^4))}\right], \quad (30)$$

where  $k = k_f \cong k_b$ , The density of the cold ensemble  $\rho_{helix}$  rotates as a "solid body" with a pitch of the  $\lambda/2$ . The speed of the axial translation is  $V_z = \lambda \cdot \delta\omega/4\pi$ .

## V. EXACT HELICAL SOLUTION

Apart from TF approximation the truly exact solution exists  $\Psi = \Psi_f + \Psi_b$  which is again a superposition of the two counter propagating *paraxial* matter waves  $\Psi_f$  and  $\Psi_b$ . Then GPE (20) is reduced to the "paraxial form" relevant to highly elongated geometry, as a *helical* one in our case:

$$i\hbar \frac{\partial \Psi_{(f,b)}(\vec{r}, t)}{\partial t} = \hat{H} \Psi_{(f,b)}(\vec{r}, t) = -i2k_{(f,b)} \frac{\hbar^2}{2m} \frac{\partial \Psi_{(f,b)}}{\partial z} + \frac{\hbar^2}{2m} k_{(f,b)}^2 \Psi_{(f,b)} - \frac{\hbar^2}{2m} \Delta_\perp \Psi_{(f,b)} + V_{opt}(z, r, \theta, t) \Psi_{(f,b)} + \frac{4\pi\hbar^2 a_s(\vec{B})}{m} |\Psi_{(f)} + \Psi_{(b)}|^2 \Psi_{(f,b)}, \quad (31)$$

Let us assume the perfect mutual cancellation of trapping and interaction terms:

$$-V_{opt}(z, r, \theta, t) \Psi_{(f,b)} = \frac{4\pi\hbar^2 a_s(\vec{B})}{m} |\Psi|^2 \Psi_{(f,b)}, \quad (32)$$

as it might happen when positive scattering length  $a_s$  provides nonlinear defocusing which is compensated by red detuned optical attraction to intensity maxima.

Taking again the exact helical solution of (32) as a superposition of the two counter-propagating vortices:

$$\Psi_{exact}(z, r, \theta, t) = \Psi_f(z, r, \theta, t) + \Psi_b(z, r, \theta, t) \cong \tilde{\Psi}_f \cdot \exp\left[i\left(-\frac{\mu_f t}{\hbar} + k_f z + \ell\theta\right)\right] + \tilde{\Psi}_b \cdot \exp\left[i\left(-\frac{\mu_b t}{\hbar} - ik_b z - \ell\theta\right)\right], \quad (33)$$

under the natural assumption  $k_{(f,b)} \partial \tilde{\Psi}_{(f,b)}/\partial z \gg \partial^2 \tilde{\Psi}_{(f,b)}/\partial z^2$  for the slow varying  $\tilde{\Psi}_{(f,b)}$  (with respect to  $z$ ), the following equation is valid:

$$i2k_{(f,b)} \partial \tilde{\Psi}_{(f,b)}/\partial z + \Delta_\perp \tilde{\Psi}_{(f,b)} = 0 \quad (34)$$

which have the vortex solutions with charge  $\ell$  for the  $\tilde{\Psi}_{f,b}(z, r)$  with initial condition at  $z = 0$  equals  $\tilde{\Psi}_0$ :

$$\tilde{\Psi}_{(f,b)} = \frac{\tilde{\Psi}_0 \cdot (r/D_0)^{|\ell|} \cdot \exp\left[-\frac{r^2}{D_0^2(1 + iz/(k_{(f,b)} D_0^2))}\right]}{(1 + iz/(k_{(f,b)} D_0^2))^2} \quad (35)$$

This preliminary analysis shows that a sufficiently large ensemble of  $N$  atoms might be trapped in a common quantum state with helical density distribution collocated with trapping interference pattern  $I_{tw}$ . The issues of dynamical stability with respect to small perturbations and thermodynamical stability from the point of view of least energy arguments deserve a further careful analysis and will be published elsewhere.

## VI. DISCUSSION

At present moment it is not clear whether above outlined solutions are close to a real quantum gas hydrodynamics which ought to be described by self-consistent solution of Cauchy problem for GPE. The one possible application of (25,27,33) might be in using them as variational ansatz for emulation of GPE [39]. Nevertheless the explicit form of solutions (25,27,33) offers a possibility to evaluate the significant macroscopic observables of the trapped ensemble.

Omitting the multivalued phase factor one may find that *funnel* solution  $\Psi_{fun}$  (25), has zero momentum  $P_z$ :

$$\langle P_z \rangle_{fun} = \langle \Psi_{fun} | -i\hbar \frac{\partial}{\partial z} | \Psi_{fun} \rangle = 0, \quad (36)$$

and zero angular momentum  $L_z$ :

$$\langle L_z \rangle_{fun} = \langle \Psi_{fun} | -i\hbar \frac{\partial}{\partial \theta} | \Psi_{fun} \rangle = 0. \quad (37)$$

On the other hand the *helical* solution  $\Psi_{helix}$  (27) has nonzero momentum  $P_z$ :

$$\langle P_z \rangle = \langle \Psi_{helix} | -i\hbar \frac{\partial}{\partial z} | \Psi_{helix} \rangle = N\hbar(k_f - k_b), \quad (38)$$

and again (!) zero angular momentum  $L_z$ :

$$\langle L_z \rangle_{helix} = \langle \Psi_{helix} | -i\hbar \frac{\partial}{\partial \theta} | \Psi_{helix} \rangle = 0. \quad (39)$$

The same expectation values  $\langle P_z \rangle_{exact} = \hbar(k_f - k_b)$  and  $\langle L_z \rangle_{exact} = 0$  has exact helical wavefunction  $\Psi_{exact}$  (33). Quantum mechanically this happens because the wavefunction in both cases is a superposition of the the partial matter waves  $\Psi_f$  and  $\Psi_b$  (33) (or  $\Psi_\ell$  and  $\Psi_{-\ell}$  (27)) having opposite and quantized (i.e. equal to  $\pm\ell\hbar$ ) mutually subtracted angular momenta. This feature looks rather counter intuitively from the point of view of classical hydrodynamics. Namely the density of atomic ensemble  $\rho_{helix} = |\Psi_{helix}|^2$  rotates as a *solid body* and it is expected to have classically the angular momentum  $L_{classical} = I_{zz} \cdot \delta\omega$ , where  $I_{zz}$  is the moment of inertia of the helical *wire* with density profile  $\rho_{helix}$  [40]:

$$I_{zz} = \int Nm |\Psi_{helix}|^2 r^2 dV = Nm \int |\Psi_{helix}|^2 r^2 r dr \cdot d\theta dz \sim \\ \sim Nm \int \exp(-r^2/D_0^2) r^{2+2|\ell|} \cdot (1 + \cos(\delta\omega t + (k_f + k_b)z + 2\ell\theta)) \cdot r dr \cdot d\theta dz \sim Nm D_0^2 (40)$$

Nevertheless due to the basic property of angular momentum, namely the *quantization* of the angular momentum in free space, the oppositely directed angular momenta cancel each other completely, because they have integer opposite values of  $\pm\ell\hbar$  [41]. On the contrary, the linear momentum is *not* quantized in free space and this leads to nonzero net *translational* momentum  $P_z$  of ensembles (27,33). The momentum  $P_z$  is small because of the smallness of the *group* velocity of the helical wavetrain  $V_z = \delta\omega/(k_f + k_b)$ . For example when frequency splitting  $\delta\omega$  is induced by rotational Doppler effect [13, 17], the speed of the axial translation of the helical density profiles (27,33) is  $V_z \sim$  several  $\mu m$  per second. The azimuthal velocity  $V_\theta = \delta\omega \cdot D_0$  is about two orders of magnitude bigger due to  $D_0/\lambda \sim 10^2$ , but rotational contribution to kinetic energy  $E_{kin}$  is zero as well as the net angular momentum of the wavetrain.

The interesting physical consequences relevant to experiments with quantum gas in optical traps may be formulated from the point of view of the Landau criterion  $|\vec{V}| > \epsilon(\vec{p})/|\vec{p}|$  for the appearance of elementary excitations (rotons) and superfluidity destruction ( $\epsilon(\vec{p})$  is the energy - momentum dispersion relation). Following to [18, 31] consider the flow of quantum gas in a narrow channel with velocity  $\vec{V} = \vec{V}_z + \vec{V}_{theta}$ . In the rest frame the momentum of excitation  $\vec{p}$  ought to be opposite to the velocity of superfluid  $\vec{V}$ , because of the least energy constraint imposed upon excitation  $\epsilon(\vec{p}) + \vec{p} \cdot \vec{V} < 0$ . Thus  $\epsilon(\vec{p}) - |\vec{p}| \cdot |\vec{V}| < 0$  and  $|\vec{V}| > \epsilon(\vec{p})/|\vec{p}|$ . Because in our case the only significant component of  $\vec{V}$  is  $V_\theta = \delta\omega D_0/2$ , the condition of appearance of excitation with momentum  $\vec{p}$  reads as:

$$\delta\omega_{crit} D_0 > 2\epsilon(\vec{p})/|\vec{p}|. \quad (41)$$

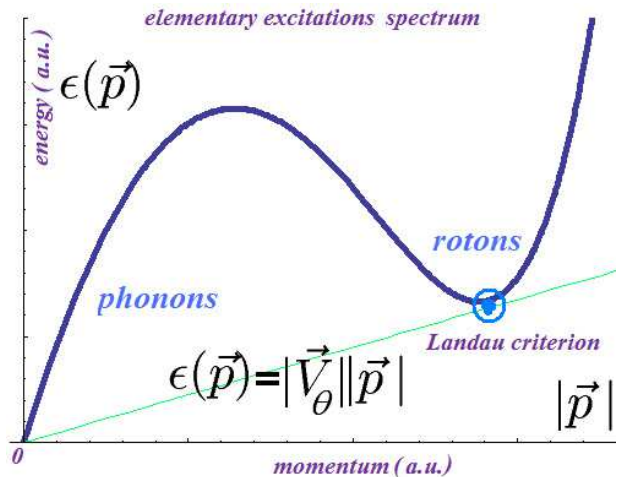


FIG. 3: Landau criterion for superfluidity for helical trap. Roton minimum touches the straight line  $|\vec{V}_\theta||\vec{p}|$  which corresponds to superfluid regime destruction by means of roton excitation.

The experimentally controllable detuning  $\delta\omega$  of counter propagating waves  $\omega_f$  and  $\omega_b$  by rotational Doppler effect, hence changing the angular velocity of helix rotation makes possible to determine the critical velocity of superfluid, defined by contact point of roton minimum of  $\epsilon(\vec{p})$  (fig. 3) with the line  $|\vec{p}|V_\theta$ .

## VII. CONCLUSION

In this paper we demonstrated the procedure of getting the analytical expressions for the macroscopic wave functions of the sufficiently large ultracold atomic ensemble which contains about  $N \cong 10^{(9-12)}$  atoms trapped by a slowly rotating helical optical potential with the rotation frequencies in the range  $\nu_{rotation} \cong 0.01 - 1 Hz$ . The helix pitch is equal to a half of the trapping wavelength  $\lambda \cong 0.8 - 10.6 \mu m$ , the helix diameter is assumed to be in the range  $D_0 \cong 30 - 100 \mu m$ , the trap length is within the Rayleigh range  $Z_r \cong 300 - 1000 \mu m$ . We formulated the necessary condition for appearance of the static helical configuration, determined by Thomas-Fermi balance of the self-defocusing of condensate with positive scattering length  $a_s$  and attractive action of the optical dipole force at "red" detuning, provided the kinetic energy is negligible (22). The minimal achievable ensemble temperature  $T_{min}$  is approximately defined by recoil energy  $k_B \cdot T_{min} = E_{recoil} = 4 \cdot \hbar^2 / (2m\lambda^2)$  [4].

The possible experimental implementation of helical trapping might be the sudden *switching on* of the helical potential after condensate release from elongated optical trap in a way similar to switching of accelerated grating in Ref. [5].

The solutions of the Gross-Pitaevskii equation were obtained in the Thomas-Fermi approximation. The helical solution  $\Psi_{helix}(z, r, \theta, t)$  with homogeneous chemical po-



tential  $\mu$  is perfectly correlated with the optical intensity  $I_{tw}(z, r, \theta, t)$  and rotates with the frequency difference of the bichromatic interference pattern  $\delta\omega$ . This solution with rotating helical density profile  $\rho_{helix}(z, r, \theta, t)$  (27) describes the two possible regime of superfluid flow. The first regime is the test of the condensate dragging by optical potential analogously to NIST rotating lattice tests [1]. In this case the condensate fragments moves together with dragging optical helix. The completely opposite regime might appear when trapped superfluid remains in rest with respect to laboratory frame because of the possible *absolute absence* of friction. This second regime is a very interesting from the point of view of actual superfluids properties when they are immersed in a nonstationary boundaries.

The solution with spatially varying chemical potential  $\mu(r)$  (26) has a stationary in time density profile  $\rho_{fun}(z, r, \theta, t)$ , looking like "funnel" whose maximum is collocated with average radius of LG beam pattern. This case (25) with nonrotating density profile  $\rho_{fun}(z, r, \theta, t)$  demonstrates the seeming absence of dragging.

An addition the formal (i.e.verified by direct substitution) exact *paraxial solution*  $\Psi_{exact}$  of GPE (33) was analyzed by calculation of *translational* momentum  $P_z = N(k_f - k_b)$  and angular momentum  $L_z = 0$ . In contrast to the classically expected motion with definite helical field of velocities  $\vec{V}$  [32] the helical solutions demonstrates nonzero translation speed along with the seeming absence of rotations ( $\langle L_z \rangle = 0$ ).

The possibility of emerging turbulence was discussed for helical geometry by virtue of the Landau criterion

$|\vec{V}| > \epsilon(\vec{p})/|\vec{p}|$ . The probable mechanism of the flow stability loss is in reaching the critical angular velocity  $\delta\omega_{cr} = 2|V_{theta}|/D_0$ .

The peculiarities of the cooling mechanisms in this helical configuration were not studied in the current work. But we hope that a *helical beam waist* (see fig.1) trapping geometry might reveal the new features of the well studied mechanisms as a the Doppler cooling [42], polarization gradient cooling [15] or velocity selective population trapping [43]. The newly found helical feature of the optical speckle patterns [44] is also a promising opportunity.

The red detuned rotating helical optical trap as is shown in sec.III and in [13] might be arranged with the aid of conventional optical elements, namely beam splitters, low curvature mirrors, spherical and cylindrical lenses. The proposed *loop* trapping geometry offers a possibility of the not only rotation detection but assembling of the cold protein-like (i.e.reminiscent to *alpha* helices) molecules as well. Noteworthy also the similar geometry of the colliding LG optical vortices of picosecond duration with opposite angular momenta which was proposed recently for the helical plasma currents excitation using dragging via ponderomotive force [32]. This mechanism of the plasma vortex excitation resembles the above shown GPE (20) with ponderomotive helical dipole potential. As the plasma vortices might be the sources of the axial magnetic fields, the superfluid motion in helical trapping environment is associated usually with a so-called *artificial* magnetic fields [45, 46].

- 
- [1] S.Tung, V.Schweikhard, and E.A.Cornell, Phys.Rev.Lett., **97**, 240402 (2006).
- [2] S.Tung, V.Schweikhard, and E.A.Cornell, Phys.Rev.Lett., **99**, 030401 (2007).
- [3] R.Grimm, M.Weidemuller and Yu.B.Ovchinnikov, Adv.At.Mol.Opt.Phys., **42**, 95 (2000).
- [4] F. Dalfovo, S.Giorgini, S.Stringari, L.P.Pitaevskii, Rev.Mod.Phys.**71**,463(1999).
- [5] M. Cristiani, O. Morsch, J. H. Muller, D. Ciampini, and E. Arimondo, Phys.Rev.A, **65**, 063612 (2002).
- [6] O.Morsch, M.Oberthaler, Rev.Mod.Phys. **78**, 179 (2006).
- [7] T. Puppe, I. Schuster, A. Grothe, A. Kubanek, K. Murr, P.W.H. Pinkse, and G. Rempe, Phys.Rev.Lett., **99**, 013002 (2007).
- [8] E.R.I.Abraham, J.Tempere and J.T.Devreese, Phys.Rev, **64A**, 023603 (2002).
- [9] A.Yu.Okulov, J.Phys.B., **41**, 101001 (2008).
- [10] M.Bhattacharya, Opt.Comm. **279**, 219 (2007).
- [11] A.Yu.Okulov, JETP Lett., **88**, 631 (2008).
- [12] M.Woerdemann, C.Alpmann and C.Denz, Opt. Express, **17**, 22791(2009).
- [13] A.Yu.Okulov, J. Opt. Soc. Am. B **27**, 2424-2427 (2010).
- [14] K.Volke-Sepulveda and R.Jauregui, J.Phys.B., **42**, 085303 (2009).
- [15] J. Dalibard and C. Cohen-Tannoudji, J. Opt. Soc. Am. B **6**, 2023 (1989).
- [16] M.O.Scully, M.S.Zubairy, "Quantum optics", Ch.17, (Cambridge University Press) (1997).
- [17] J. Arlt, M. MacDonald, L. Paterson, W. Sibbett, K. Volke-Sepulveda and K. Dholakia, Opt. Express, **10**(19),844(2002).
- [18] I.M. Khalatnikov, "An Introduction to the Theory of Superfluidity", Perseus Publishing, Cambridge, MA, (2000).
- [19] A.L.Fetter, Rev.Mod.Phys. **81**, 647 (2009).
- [20] A.Yu.Okulov, J.Mod.Opt., **55**, 241 (2008).
- [21] Y.F.Chen, Y.P.Lan, Phys.Rev.A, **64**, 063807 (2001).
- [22] K.Staliunas, C.O.Weiss, J. Opt. Soc. Am. B **12**, 1142 (1995).
- [23] G.Ruben, D.M.Paganin, M.J.Morgan, Phys.Rev.A, **99**, 013002 (2008).
- [24] S.Giorgini, L.P.Pitaevskii, S.Stringari, Rev.Mod.Phys. **80**, 1215 (2008).
- [25] I.Bloch, J.Dalibard, W.Zwinger, Rev.Mod.Phys. **80**, 885 (2008).
- [26] B.Damski, H.Fehrmann, H.H.Everts, M.Baranov, L.Santos and M.Lewenstein, Phys.Rev.A **72**, 053612 (2005).
- [27] N.G.Basov, I.G.Zubarev, A.B.Mironov, S.I.Mikhailov and A.Y.Okulov, JETP, **52**, 847(1980).
- [28] J.Leach, M.J.Padgett, S.M.Barnett, S.Franke-Arnold, and J.Courtial, Phys.Rev.Lett., **88**, 257901 (2002).
- [29] B.Y.Zeldovich, N.F.Pilipetsky and V.V.Shkunov "Prin-

- principles of Phase Conjugation*", Ch.2 (Berlin:Springer-Verlag )(1985).
- [30] A.V.Mamaev, M.Saffman and A.A.Zozulya, Phys.Rev.A, **56**, R1713 (1997).
- [31] R.P.Feynman, "*Statistical mechanics*", (Ch.11, Reading, Massachusetts,1972).
- [32] A.Yu.Okulov, Phys.Lett.A, **374**, 4523-4527 (2010).
- [33] E.M.Lifshitz, L.P.Pitaevskii and V.B.Berestetskii, "*Quantum Electrodynamics*", Butterworth-Heinemann, Oxford § 6,8 (1982).
- [34] S.M.Barnett, J.Mod.Opt., **57**, 1339-1343 (2010).
- [35] J.E.Sipe, Phys.Rev.A, **52**, 1875 (1995).
- [36] V.S.Lieberman and B.Y.Zeldovich, Phys.Rev.A, **46**, 5199 (1992).
- [37] L.Allen, M.W.Beijersbergen, R.J.C.Spreeuw and J.P.Woerdman, Phys.Rev.A, **45**, 8185-8189 (1992).
- [38] K.Yu.Bliokh and Yu.P.Bliokh, Phys.Rev.Lett., **96**, 073903 (2006).
- [39] B.A.Malomed "*Variational methods in nonlinear fiber optics and related fields*", Progress in Optics, **43**, 69-191 (E.Wolf, Editor: North Holland, Amsterdam )(2002).
- [40] L.D. Landau and E.M. Lifshitz, "*Mechanics*", Butterworth-Heinemann, Oxford (1976).
- [41] M. F. Andersen, C. Ryu, P. Clade, V. Natarajan, A. Vaziri, K. Helmerson, W. D. Phillips, Phys. Rev. Lett., **97**, 170406 (2006).
- [42] V.S.Letokhov, JETP Lett., **7**, 272 (1968). T. W. Hansch and A. L. Schawlow, Opt. Commun. **13**, 68 (1975).
- [43] A. Aspect, E. Arimondo, R. Kaiser, N. Vansteenkiste, and C. Cohen-Tannoudji, Phys.Rev.Lett., **61**, 826-829 (1988).
- [44] A.Yu.Okulov, Phys.Rev.A, **80**, 013837 (2009).
- [45] C.Nayak, S.H.Simon, A.Stern, M.Freedman, and S.D.Sarma, Rev.Mod.Phys. **80**, 1083-1159 (2008).
- [46] "Colloquium: Artificial gauge potentials for neutral atoms". J.Dalibard, F.Gerbier, G.Juzeliunas, P.Ohberg, Submitted to RMP, arXiv:1008.5378(2010).